Urban Surroundings Influence on Air Temperature in a Small Urban Area of Curitiba-Brazil

Cristiane Rossatto Candido, Francine Aidie Rossi

Civil Construction Engineering Postgraduate Program, Federal University of Paraná, Curitiba, Brazil
Email: rossattoc@gmail.com

Abstract

The formation of urban climates constitutes a distinctive system intrinsically linked to the urban environment. This study aims to delve into the impact of the urban environment on climatic variables. The Urban Weather Generator (UWG) algorithm was employed to generate climatic data, facilitating the creation of an epw climate file that corresponds to the urban characteristics surrounding the Centro Politécnico campus at the Federal University of Paraná (UFPR). Comprehensive analyses encompassing land use, occupancy patterns, albedo, surface absorption, anthropogenic heat, and architectural attributes were conducted. A comparative assessment between the UWG-derived air temperature values and meteorological station data revealed that the UWG effectively characterizes the air temperature patterns around the UFPR campus. The anticipated air temperature values consistently surpass the original dataset (SWERA), which was utilized as input, primarily during the hours from 3 p.m. to 7 a.m., showcasing the unmistakable urban heat island phenomenon.

Keywords

Urban Weather Generator, Air Temperature, Urban Surroundings

1. Introduction

Cities represent intricate systems, and climatic patterns within them are shaped by a myriad of factors encompassing soil occupancy, urban canyon geometry, vegetated regions, water bodies, anthropogenic heat, and bioclimatic urban planning. Consequently, these factors induce modifications in the microclimate, thereby manifesting the discernible impacts of urban heat islands and the

greenhouse effect.

As per the Brazilian Panel for Climate Change (PBMC), diverse Brazilian biomes exhibit indicators pointing towards temperature escalation, spanning from 2.5˚C to 6˚C, by the conclusion of the 21st century [1]. Additionally, in accordance with the PBMC, projections foresee a rise in the global urban population from 64% to 69% by 2050 [1]. Hence, proactive intervention and meticulous scrutiny of urban climatic variables, notably air temperature, become imperative.

Fluctuations in air temperature within urban settings are intrinsically linked to broader global dynamics, their amplitude commensurate with the modus operandi of urbanization. Notably, escalating air temperatures also exert tangible influences on building performance.

Evaluating the thermodynamic performance of buildings mandates the utilization of climate data. However, the selection of these data cannot be arbitrary, as they must accurately encapsulate the climatic nuances of the chosen locale. Moreover, haphazardly chosen data may engender inappropriate climate loads for the subject building. The consensus suggests that a minimum dataset spanning a decade [2] is requisite to enable effective analysis and the subsequent generation of a weather file.

In addition, the data chain available for analyzing and generating weather files mostly originates from meteorological stations located in rural areas. This creates a challenge when attempting to assess climate conditions in specific microregions, which directly impact the thermal comfort of pedestrians and inhabitants.

Several studies aiming to align urban environments with building energy simulations are associated with the Urban Weather Generator (UWG) algorithm [3] [4]. The program generates a new weather file based on the characteristics of the urban surroundings. Within the input climate file, the algorithm updates climate variables such as air temperature, air humidity, and radiant temperature. The resulting file is in the epw format and is utilized in building performance simulations. Changes in climate variables occur because of information input into the algorithm, which is related to the urban context surrounding the building or urban climate station [5] [6].

Overall, the text is clear and conveys the intended message effectively. The adjustments made mainly focus on enhancing the readability and coherence of the content.

The references [7] and [8] conducted studies utilizing the Urban Weather Generator (UWG) to examine the impact of solar radiation on urban climate and its consequent effect on the thermal load of commercial buildings in two Brazilian cities: Maceio/AL and Santa Maria/RS. Findings from [7] reveal that there is a reduction in cooling load ranging between 16% and 18% when considering urban geometry with shading in the context of Maceio's climate. Meanwhile, reference [8] demonstrated that the heat island effect in Santa Maria leads

to a 5% to 59% increase in refrigeration thermal load.

The reference [9] investigated the energetic performance of constructions, factoring in climate phenomena such as the heat island and solar obstruction, across ten distinct case studies in Rome (Italy) and Antofagasta (Chile). The outcomes underscore that urban shading plays a pivotal role in mitigating refrigeration energy consumption in warm climates, and the urban heat island effect is more pronounced in temperate climates.

Consequently, leveraging the modified weather file, which considers the building's surroundings, may contribute to attaining more dependable thermal and energetic outcomes. This approach enables a more effective implementation of measures aimed at reducing energy consumption. This study assesses the influence of the urban environment on weather fluctuations, based on data collected from a weather station situated outside the urban area in Curitiba, by scrutinizing average air temperature values.

2. Objective

This research aims to investigate the impact of urban surroundings on the behavior of air temperature within a localized section of a neighborhood in Curitiba, Brazil.

3. Approach

The Urban Weather Generator (UWG) software was employed to assess the influence of urbanization on climate variables. The requisite input data, designated as reference data, encompass soil classification, facade area percentage, constructed area percentage (occupancy rate), building height, and thermal characteristics of both natural and construction materials.

Soil classification was accomplished through the utilization of the Geographic Information System (GIS), specifically QGIS, along with the Semi-Automatic Classification Plug-in (SCP) for soil classification.

The percentages of building constructed areas were acquired from 3D maps accessible at https://cadmapper.com/. This online platform facilitates the conversion of publicly available geospatial data, including OpenStreetMap and NASA datasets, into CAD and SketchUp files.

Data pertaining to building and material thermal attributes were sourced from Brazilian standards and scholarly articles.

3.1. Climate Profiling

As per the Köppen-Geiger climate classification, Curitiba is characterized by a temperate maritime humid climate (Cfb) [10] renowned for its substantial precipitation levels and mild temperatures. In accordance with Brazilian bioclimatic zoning, Curitiba falls within Bioclimatic Zone 1 [11] and holds the distinction of being Brazil's coldest capital city. The annual average temperature stands at 19.7°C, with the warmer months spanning January and February, featuring av-

erage temperatures ranging from 17°C to 20°C. Conversely, the colder months of June and July exhibit average temperatures between 12°C and 14°C. Notably, daily temperature fluctuations can extend to 25.7°C.

3.2. Study Area

To assess microclimate variations, comparisons were made between air temperature measurements from an urban and a rural locale. [12], utilizing the TRY method, identified noteworthy disparities in air temperature data obtained from the SIMEPAR (Parana Meteorological System) and Afonso Pena Airport meteorological stations. As a result, this study centers its attention on the vicinities surrounding these two stations, with the SIMEPAR station representing the urban environment and the Afonso Pena Airport station delineating the rural context.

The SIMEPAR meteorological station (depicted in Figure 1(a)) is situated in the Jardim das Américas neighborhood within the Centro Politécnico campus of the Federal University of Paraná (UFPR). This residential neighborhood is characterized by predominantly low-rise structures, with approximately 99% of buildings comprising up to two floors.

In contrast, the Afonso Pena Airport is located in São José dos Pinhais city, proximate to Curitiba, and its associated meteorological station is classified as a rural area. Figure 1 illustrates the designated analysis zones for the two selected points. Land use within the chosen sector of Jardim das Américas exhibits heterogeneity, encompassing remnants of native forest, low-rise built structures, extensive grassy areas, and a section of urban roadway with high vehicular traffic.

The impact of soil occupancy on microclimate was examined within a specified influence radius. As outlined by reference [13], the extent of the influence radius varies across studies, typically ranging from 100 to 500 meters. In this research, a radius of 350 meters was adopted for both the rural and urban areas, drawing upon the insights of [5] and [9]. The selection of this value considered diverse land use factors, encompassing the constructed area ratio within the Jardim das Americas and UFPR Polytechnic Center Campus neighborhoods, as

(a)   (b)

Figure 1. Surrounding map from (a) SIMEPAR meteorological station e (b) Afonso Pena Airport station (drown up from Open Street Map image-2020).

well as the presence of native vegetation within the UFPR Polytechnic Center Campus reserve.

3.3. Land Use and Occupation

Four distinct land use categories were delineated for soil classification: asphalt, constructed area (occupancy rate), arboreal vegetation, and low vegetation. In order to input these data into the UWG, it was imperative to ascertain the corresponding percentages associated with each land use type.

To achieve this, Sentinel-2 satellite imagery was harnessed, complemented by the utilization of Geographical Information Systems (GIS), specifically QGIS. Within the QGIS framework, the Semi-automatic Classification (SCP) plugin was integrated, which facilitated the process of soil classification. The ensuing sections elucidate the methodologies employed to derive land use and occupation maps, actual constructed area representations, and facade area mappings for the targeted area of investigation, specifically the delimited segment of the Jardim das Américas neighborhood (as depicted in Figure 1(a)).

3.3.1. Procedure 1: Satellite Images Preparation

Sentinel-2 satellite images were employed for land use classification. This satellite sensor is optoelectronic and multispectral, featuring a resolution range of 10 to 60 meters across the shortwave infrared, near infrared, and visible infrared spectral regions. With its 13 spectral channels, the sensor effectively captures variations in vegetation, encompassing temporal changes and mitigating the potential impact of atmospheric conditions on image quality [14]. The distinctive image bands of Sentinel-2, along with their specific characteristics, are delineated in Table 1.

Table 1. Bands from sentinel-2 images (Adapted from [14]).

Band	Wavelength (μm)	Resolution (m)
Band 1 – Coastal aerosol	0.443	60
Band 2 – Blue	0.490	10
Band 3 – Green	0.56	10
Band 4 – Red	0.665	10
Band 5 – Red Edge 1	0.705	20
Band 6 – Red Edge 2	0.740	20
Band 7 Red Edge 3	0.783	20
Band 8 – near infrared (NIR)	0.842	10
Band 8A – Red Edge 4	0.865	20
Band 9 – Water Steam	0.945	60
Band 10 – Cirrus	1.375	60
Band 11 – SWIR	1.610	20
Band 12 – SWIR	2.190	20

Considering the designated influence radius of 350 meters, images with resolution bands of 10 meters were selected for use, specifically bands 2, 3, 4, and 8 (Table 1). These images were sourced from the US Geological Services (USGS) and were specifically chosen to ensure cloud coverage of under 10%. Notably, the images utilized are Level-2A, pertaining to surface reflectance [14].

Upon importing the image bands into the QGIS software, a process of dark object subtraction was executed, following the methodology proposed by reference [15] This correction procedure is deemed essential due to the presence of completely shadowed pixels within the images, with the received radiation in the images stemming from atmospheric scattering effects.

3.3.2. Procedure 2: Classification of Land Use by Semi-Automatic Classification Plug In

The land use and occupation were classified using the plug in developed by [14] for the QGIS software named SCP (Semi-automatic Classification). THE SCP is capable of classifying land use and occupation on a supervised manner. This procedure enables the identification of different materials in the satellite images, based on different image bands (spectral signatures). The procedure steps are described below:

1) Values conversion to raster: after atmospheric correction for the selected bands (bands 2, 3, 4 and 8), the band set is created to be used in the SCP, named as Band Set. The vector conversion to raster is done with the corrected set band, using the conversion type Center of Pixels. Reference [14] explains that during the conversion process, the vector is compared to the reference raster and output scan pixels are attributed to it, since the pixels center is inside the polygon. This polygon refers to the used satellite images.

2) Study areas cutout: taking the raster as reference, image cutout was made from images that represented the study area. First, it was used the raster SCP cutout tool to obtain the area cutout for Afonso Pena Airport and the SIMEPAR station urban surrounding. The SCP allows many raster cutouts at once, which enhances the cutout task. However, by using this feature it is only possible to cut the image in rectangular forms. This way, after soil classification it was necessary to cut the rectangles into circles.

3) ROI (Region of interest) definition: this tool classifies different materials with different spectral signatures. According to [14] each ROI is identified by a class identity, being attributed to a soil coverage class, this last one being a macro class identifier. This ROI distinction is important because it is through creating different area classes, e. g. roof area, that the constructed area macro class result is obtained. The identifiers created on this research are: a) Arboreal Vegetation; b) Low Vegetation; c) Constructed Area (referring to edification) and d) Paved Area (referring to asphalt). In this process, numerous ROI are created for each macro class. Still, it is possible to attribute name and color into the macro class identities.

4) Algorithm classification: the classification algorithm is used to generate the

land use map. According to [14] the classification algorithm compares different pixels spectral characteristics from each image to the identities attributed to the macro classes. Moreover, in accordance with [14] the SCP plug-in has three classification algorithms, being: a) Shortest Distance, which calculates the Euclidean distance amongst pixels spectral signature; b) Maximum Likelihood, estimates de probability of a pixel to belong to a soil class coverage, applying the Bayes theorem, and c) Spectral Angle Mapping, which calculates the angle between diverse image pixels spectral signatures and from spectral signatures characterized by ROI attributed by the operator. For this research the two most indicated urban surrounding methods indicated by [14] have been tested: Maximum Likelihood and Spectral Angle Mapping. The conclusion is that the most accurate method to study reality (as of the local reality visual comparison) is the Spectral Angle Mapping, being the one to be used.

3.3.3. Procedure 3: Obtaining Constructed Area Rate, Façade Area Rate and Building Height

According to [16] and [9] other necessary parameters to compose the UWG programming file are: 1) Constructed area rate: occupancy rate related to the studied total area (influence radius of 350 m); 2) Building average height, referring to the building inside the influence radius; and 3) Façade area rate.

These parameters have been obtained from the urban geometry provided by the CADMAPPED website. This tool turns data from open sources such as OpenStreetMap and Nasa into diverse modelling drawing software's files, such as AutoCAD and SketchUp. The web site offers, at no charge, up to one squared kilometers of material.

In the CADMAPPER file from the SIMEPAR weather station was drawn the influence radius (350 m) and the urban surroundings building area polygons were selected as shown in **Figure 2**.
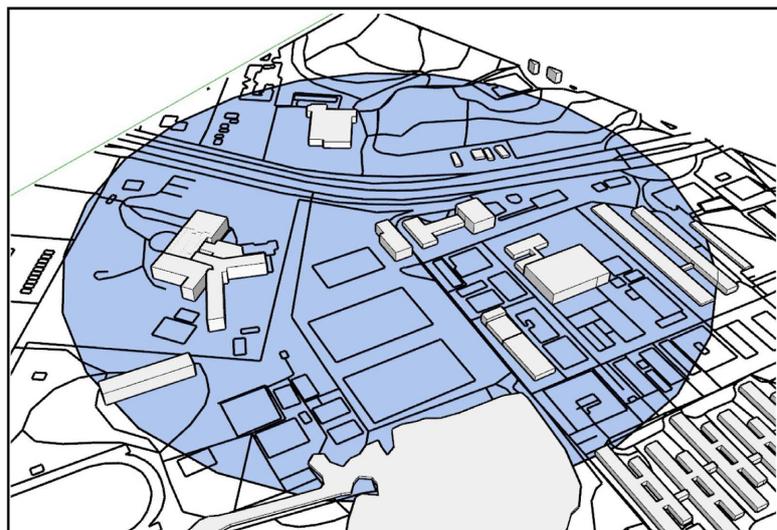
Figure 2. SIMEPAR urban surrounding influence area—Jardim das Américas Neighborhood.

Subsequently, an occupancy rate was obtained. A visual analysis was made to correct some pixel inconsistency between building areas pixels and paved area pixels (asphalt). The occupancy rate of the area is 164238.8 m² which represents 43% of the influence area.

The building average height was measured by using the 3D geometry, obtained through CADMAPPER. It can be seen, in Figure 2, that some buildings do not have a 3D model, but only its occupied area projection. This way, a Google Earth Pro tool which measures 3D distances has been applied. As attested by [17], the difference between *in loco* and Google Earth Pro measure tool is approximately 2%. The building average height obtained by the 3D measure is 6.8 meters.

Lastly, the façade area rate has been calculated from the 3D model presented in Figure 2 and the 3D Google Earth Pro measurement tool was applied. The façade area rate of the area is of 13% (50737.35 m²) of the influence area.

3.4. Urban Weather Generator (UWG) Entry File Development

The Urban Weather Generator (UWG) is a software that changes standard climate file meteorological data (epw), used in building thermo energetic simulations, into an epw file associated to microclimate conditions of a specific urban surrounding [16]. This study uses the software version V4, without graphic interface. It was generated an entry data file, in xml, with information of urban parameters of Jardim das Américas neighbourhood (Table 2) and microclimatic data from Afonso Pena meteorological stations considered as a reference weather station. The climate file used was the SWERA 838,400 and it is available online.

The entry values used in the UWG programming file are presented in Table 2. In the last column presents the research source for applied values. The arboreal low vegetation rate, constructed area rate, asphalt rate, façade area rate and building height values have been obtained by the procedures described in the previous sections.

3.5. Data Processing

The UWG generates a weather file with 8760 hourly data. In this paper is present the analysis of air temperature. It was made a comparative analysis between three data sources of air temperature: 1) the data generated by UWG. 2) the data from Afonso Pena Airport weather station (SWERA 838,400) and 3) the 2008 data from SIMEPAR weather station [12].

The average air temperature values for each month from each of the three data sources were analyzed. Also, it was analyzed the hourly average air temperature of the months that showed the highest and the lower average air temperature, respectively, February and June.

Test T was applied to verify the relation between the UWG weather file average air temperature data and the data from the airport meteorological station

Table 2. UWG entry parameters.

	Parameter	Used value	Unit	Reference
Urban area	Anthropogenic street heat	10.79	W/m^2	[18] and [19]
	Asphalt emissivity	0.92		[20]
	Asphalt albedo	0.3		[20]
	Low vegetation albedo	0.16		[21]
	Dense vegetation albedo	0.12		[21]
	Arboreal vegetation rate	0.18	% decimal	SCP Calculated
	Low vegetation rate	0.28	% decimal	SCP Calculated
	Constructed area rate	0.40	% decimal	Calculated
	Asphalt Rate	0.11	% decimal	Calculated
	Façade area rate	0.13	% decimal	Calculated
	Building average height	6.8	m	Calculated
Roof	Concrete slab roof emissivity	0.87		[22]
	Dark concrete slab albedo	0.21		[22]
	Thermal Conductivity	1.78	W/mk	calculated based on [11]
	Thermal Inertia	1753.13	kJ/m^{3}K	calculated based on [23]
	Thickness	0.32	m	Estimated
	Vegetation	0		Estimated
	Slope	0.08	unit	Estimated
	Initial temperature	20	˚C	Program default
Wall	Emissivity	0.92		[20]
	Albedo	0.4		[20]
	Thermal Conductivity	1.18	W/mK	calculated based on [11]
	Thermal Inertia	1120	kJ/m^{3}K	calculated based on [23]
	Thickness	0.15	m	Estimated
	Vegetation	0		Program default
	Slope	0		Program default
	Initial temperature	20	˚C	Program default
Glass	Albedo	0.4		[20]
	Thermal Conductivity	1.18	W/mk	calculated based on [11]
	Thermal Inertia	1120	kJ/m^{3}K	calculated based on [23]
Rural area	Thickness	0.15	m	Estimated
	Vegetation	0		Program default
	Slope	0		Program default
	Initial temperature	20	˚C	Program default
	Low vegetation rate	0.72	% decimal	Calculated

(SWERA 838,400). It was analyzed the data set of 8760 hours. The null hypothesis tested the equality of the average values of air temperatures recorded by the airport and generated by the UWG with a statistical significance of 5%.

4. Results and Discussion

The results presented in the next sections are divided into two parts. The first one shows the land use classification results and the data correction for the constructed area rate. The second part analyzes the air temperature differences for the SWERA weather file, the UWG modified weather file and for the data originated from the SIMEPAR meteorological station.

The UWG file was generated by the SWERA data set (Aeroporto Afonso Pena). The SIMEPAR weather station is in Centro Politécnico of Federal University of Paraná, in the same urban environment for which the UWG file was generated.

4.1. Land Use

Figure 3 shows the land use maps of the surroundings of Afonso Pena and SIMPEPAR meteorological stations. The maps were made using QGIS software. **Figure 3(a)** shows the different land occupation around Afonso Pena Airport meteorological station, the land uses, and their respective percentage are: low vegetation (68%), paved area (23%), arboreal vegetation (4%) and constructed area (5%).

Figure 3(b) presents the land occupation for the SIMEPAR meteorological station urban surrounding. For this area the land occupation is composed by arboreal vegetation (18%), low vegetation (28%), constructed area (33%) and paved area (21%).

4.2. Air Temperature Results

The null hypothesis tested the equality of the average values of air temperatures recorded by the airport (SWERA) and generated by the UWG with a statistical

(a)　　　　　　　　　　　(b)
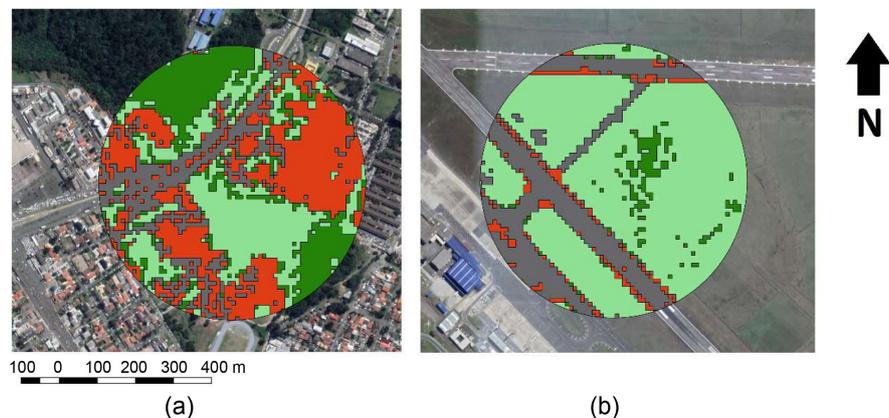
Figure 3. Surrounding soil use map for (a) Afonso Pena Airport meteorological station and for (b) SIMEPAR meteorological station (Drawn up based on a Sentinel-2 image).

significance of 5%. The results (Table 3) show that the values of air temperature from the SWERA file are different from the values generated by UWG (p-value = 0).

Figure 4 shows the correlation between the dataset of air temperature of SIMEPAR and the UWG epw file. The correlation is high despite the differences between the air temperature data. The SIMEPAR data file corresponds to the test reference year of 2008 [12], and was obtained applying the ASHRAE methodology for a period of 15 years (2002/2016). The UWG file is derived to the SWERA 838,400 file, from the Airport Afonso Pena and corresponds to the year 2012. The SWERA file is not a typical or a reference year, and the values of air temperature cannot represent mild events.

Table 3. T test for SWERA e UWG air temperature (test based on [24]).

	Ta SWERA	Ta UWG
Average	17.171	18.291
Variation	25.449	22.387
Observations	8760	8760
Pearson correlation	0.934	
Average difference hypothesis	0	
gl	8759	
Stat t	−57.964	
P (T ≤ t) uni-caudal	0	
t critical uni-caudal	1.645	
P (T ≤ t) bi-caudal	0	
t critical bi-caudal	1.960	
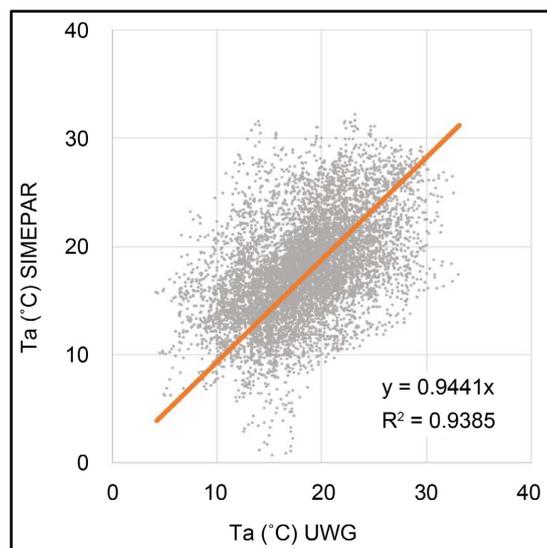
Figure 4. Correlation between UWG and SIMEPAR air temperatures.

The average monthly air temperatures of each data set are presented in Table 4. Monthly average air temperature data were used to verify the hottest (February) and coldest (June, July and August) months. The hottest month is February, in all three sample cases. The coldest month is June for the data from Afonso Pena airport and SIMEPAR and July and August (both with 14.55˚C) for the data generated by UWG.

The hottest and the coldest month for each data set were selected to analyze the differences between the different sources. This analyze was made from the hourly average air temperature. The hourly average air temperatures for February are presented in Figure 5. The biggest difference was 1.95˚C for the 8 p.m. (Ta UWG – Ta SIMEPAR). The highest value of air temperature was registered at 3 p.m. (25.58˚C) for UWG data set. The three sets of air temperature data had little difference between 9 a.m. and 2 p.m. (average difference of 0.38˚C).

Besides that, it was possible to verify that from 2 p.m. to 8 a.m. average air temperatures values from the UWG weather file are higher, possibly because capacity of the algorithm predicts the urban surrounding heat island tendency. as pointed out by [16] and [5]. Furthermore, it is important to emphasize that weather files are created with representative data that do not consider months and years that present typical behavior, excluding extremes values.

However, for June (Figure 6), the UWG weather file variation is higher when compared to the SIMEPAR meteorological station data. The average temperature

Table 4. Dry bulb temperatures classified by color.

Month	Jan	Feb	Mar	Apr	May	Jun	Jul	Aug	Sep	Oct	Nov	Dec
						Air temperature average (˚C)						
Swera epw	20.94	21.06	20.05	18.69	14.93	13.14	13.55	13.28	15.26	16.84	18.77	19.83
UWG epw	21.93	21.98	21.02	19.71	16.6	15.02	14.55	14.55	15.98	17.76	19.78	20.87
Simepar data	20.04	21.30	20.38	18.45	15.65	14.28	16.03	16.36	15.16	18.15	18.49	20.01
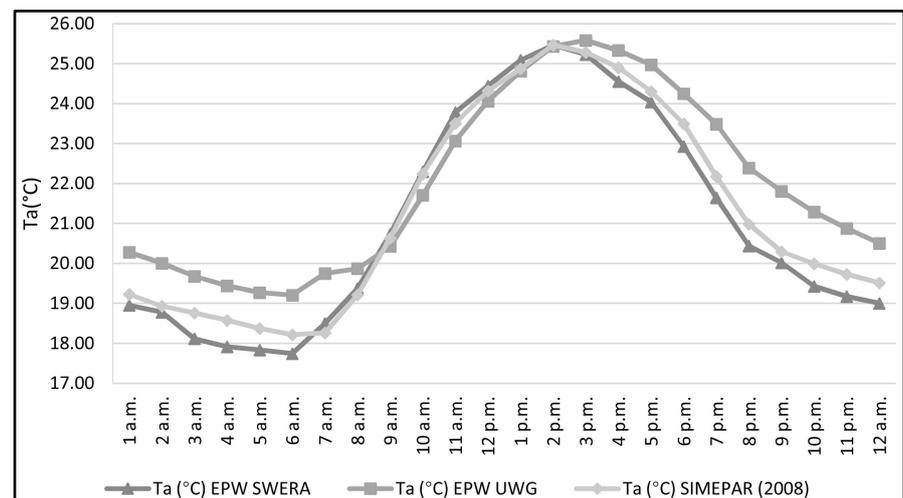
Figure 5. Hourly average air temperature for February.
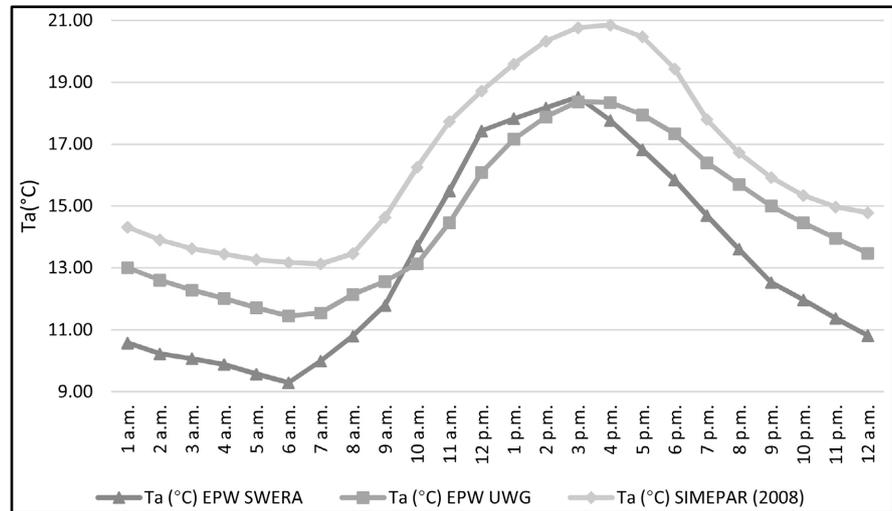
Figure 6. Hourly average air temperature for June.

is, respectively, 20.85°C and 18.35°C, for the SIMEPAR meteorological station and the UWG weather file, at 4 p.m. This way, it is important to reinforce the conclusion of [5] that the meteorological station measurement might be influenced by urban surrounding close to the thermometer and that, even though UWG is a suitable tool to predict the urban morphology impacts on climate variables, the accuracy can be affected by peculiar parameters. In the authors research the influence of sea breeze was not predicted by UWG.

When evaluating the hourly average difference between the SWERA and UWG weather files (Table 4), it is shown that the UWG algorithm predicted a risen temperature at the evaluated urban surrounding. It is important to emphasize that the SWERA weather file is from a meteorological station outside the urban mesh.

The analysis of a specific summer day (February 14) and winter day (June 15) shows that the UWG air temperature behavior is closer to the SIMEPAR air temperature than the SWERA data. The data for February 14 (summer) are presented in Figure 7. Even though there is a difference between SIMEPAR data and UWG weather file, the behavior of the UWG air temperature is closer to the SIMEPAR data than the SWERA data. It means that the UWG predicted the behavior of the urban environment. The urban environment heating starts at the beginning of the morning, concurring with the solar incidence period and prevails to the beginning of the night, when the temperature tends to slowly drop.

SIMEPAR data have been used as UWG temperature behavior generated data verification. It must be emphasized that the entry data for the UWG algorithm are dated from 2012, while the ones from SIMEPAR are referred to the test reference year of 2008.

All the same, for the winter day data (June 15) it was possible to understand the hourly air temperature behavior for the surrounding analyzed in Curitiba when comparing it to the one from the UWG and SIMEPAR temperature curves behavior (Figure 8). Temperature values increase from 9 a.m. and reach its peak
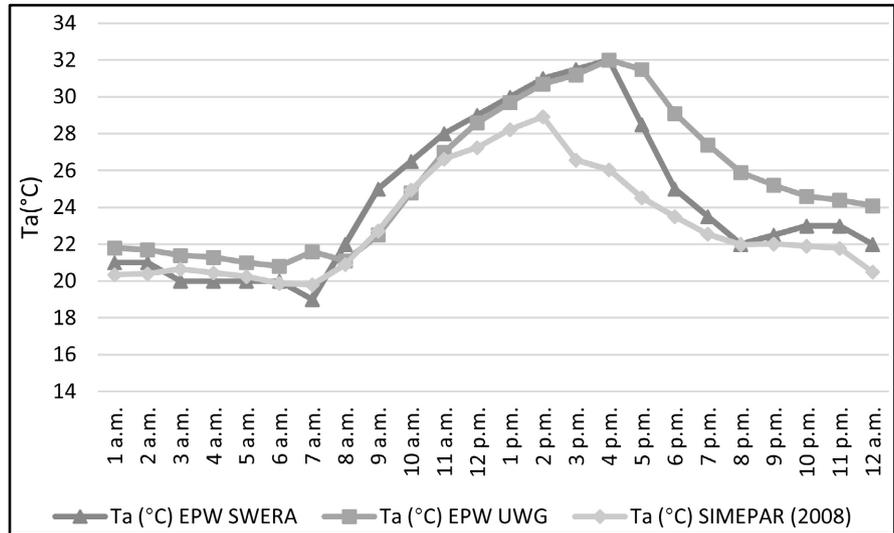
Figure 7. Hourly air temperature for a typical summer day—February 14.
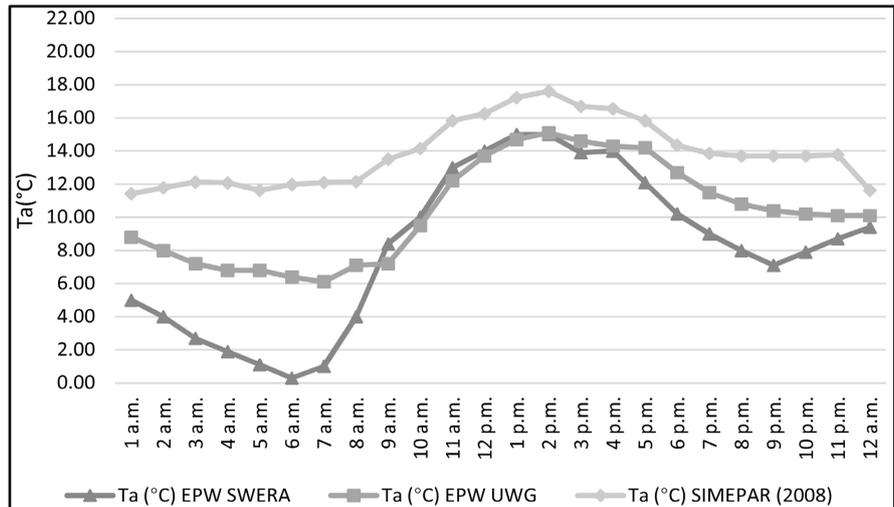
Figure 8. Hourly average air temperature for a typical winter day—June 15.

between 1 p.m. and 4 p.m. After 4 p.m. the temperature drops, but not much, which can be explained by the effect of incident solar radiation on urban surfaces, especially the ones coming from buildings and pavements. This effect maintains the urban area temperature higher.

Once more it is possible to verify that the behavior of the temperatures predicted by the UWG algorithm is like the temperature of SIMEPAR.

5. Conclusions

This research presented the urban surroundings' influence over air temperature behavior in a small portion of a neighborhood in Curitiba/Brazil. A new set of temperature data was generated by applying the Urban Weather Generator (UWG) algorithm from the data weather station of Afonso Pena Airport (rural weather station—SWERA 838400). The UWG prediction was compared with

data from the SIMEPAR weather station (TRY 2008).

As stated in other studies like [4] and [5] the difference between values generated by UWG and SIMEPAR data (TRY 2008) might be the result of the decrease in the efficiency of the UWG for urban areas with different uses and occupation densities. That is the case for the urban surrounding at the SIMEPAR meteorological station, in which the vicinity (analyzed radius of 350 meters) is characterized by a forest reserve, the UFPR Campus and part of a predominantly residential Jardim das Americas neighborhood.

Another possible explanation for the differences between UWG generated values and the SIMEPAR data is the dataset itself. The SIMEPAR data are from the test reference year (TRY) of 2008, while the SWERA data file is from 2012. While one base (SIMEPAR) refers to an average meteorological year, the other (SWERA) refers to data from a specific year.

Despite of the complexity of the analyzed area (different uses and constructed density), the UWG algorithm was able to predict the behavior of the air temperature. A comparison of air temperature predicted by UWG with data from SIMEPAR shows consistency in the behavior of air temperature, both for monthly average data and for daily hourly data.

The daily air temperature data have shown that the values of air temperature predicted by the UWG represent the air temperature behavior for both summer and winter days in Curitiba.

It is indicated that further studies are carried out evaluating the other variables such as radiant temperature and relative humidity, as well, evaluating other urban areas of Curitiba.

Acknowledgements

Conflicts of Interest

The authors declare no conflicts of interest regarding the publication of this paper.

References

[1] Climate Change Brazilian Pannel (PBMC) (2016) Mudanças climáticas e cidades: Relatório Especial do Painel brasileiro de mudanças climáticas. http://www.pbmc.coppe.ufrj.br/documentos/Relatorio_UM_v8_sumario-executivo.pdf

[2] American Society of Heating, Refrigerating and Air-Conditioning Engineers (ASHRAE) (2010) STANDARD 90.1. Energy Standard for Buildings except Low-Rise Residential Buildings. ASHRAE: Atlanta.

[3] Jalali, Z., Shamseldin, A.Y. and Ghaffarianhoseini, A. (2024) Urban Microclimate Impacts on Residential Building Energy Demand in Auckland, New Zealand: A

Climate Change Perspective. *Urban Climate*, **53**, 1-14.
https://doi.org/10.1016/j.uclim.2024.101808

[4] Yin, S., Xiao, S., Ding, X. and Fan, X. (2024) Improvement of Spatial-Temporal Urban Heat Island Study Based on Local Climate Zone Framework: A Case Study of Hangzhou, China. *Building and Environment*, **248**, 1-14.
https://doi.org/10.1016/j.buildenv.2023.111102

[5] Salvati, A., Roura, H.C. and Cecere, C. (2016) Urban Heat Island Prediction in the Mediterranean Context: An Evaluation of the Urban Weather Generator Model. *ACE*: *Architecture*, *City and Environment*, **11**, 135-156.
https://doi.org/10.5821/ace.11.32.4836

[6] Chiesa, G. and Palme, M. (2018) Valutare la vulnerabilità urbana ai cambiamenti climatici e alle isole di calore urbano. *TECHNE*, **15**, 237-245.

[7] Lima, I.; Scalco, V.; Lamberts, R. (2019) Estimating the Impact of Urban Densification on High-Rise Office Building Cooling Loads in a Hot and Humid Climate. *Energy and Buildings*, **182**, 30-44. https://doi.org/10.1016/j.enbuild.2018.10.019

[8] Machado, R.M.S. (2019) Modelagem do impacto da ilha de calor urbano sobre o desempenho energético de escritórios condicionados artificialmente. Master's Dissertation, Universidade Federal de Santa Catarina, Florianópolis.

[9] Salvati, A., Palme, M., Chiesa, G., Kolokotroni, M. (2020) Built Form, Urban Climate and Building Energy Modelling: Case-Studies in Rome and Antofagasta. *Journal of Building Performance Simulation*, **1**, 1-17.
https://doi.org/10.1080/19401493.2019.1707876

[10] Peel, M., Finlayson, B. and Mcmahon, T. (2007) Updated World Map of the Koppen-Geiger Climate Classification. *Hydrology and Earth System Sciences*, **11**, 1633-1644. https://doi.org/10.5194/hess-11-1633-2007

[11] Brazilian Association of Technical Normatives (Associação Brasileira de Normas Técnicas—ABNT) (2003) NBR 15.220—Parte 3: Zoneamento bioclimático brasileiro e diretrizes construtivas para habitações unifamiliares de interesse social.
https://edisciplinas.usp.br/pluginfile.php/5660736/mod_folder/content/0/NBR%2015220/NBR15220-3.pdf

[12] Candido, C.R. and Rossi, F.A. (2019) Ano climático de referência para curitiba: Comparação entre dados de duas estações.
https://eventos.antac.org.br/index.php/encac/article/view/4014

[13] Oke, T.R. (2006) Initial Guidance to Obtain Representative Meteorological Observations at Urban Sites.
http://www.wmo.int/pages/prog/www/IMOP/publications/IOM-81/IOM-81-UrbanMetObs.pdf

[14] Congedo, L. (2012) Semi-Automatic Classification Plugin Documentation.
https://semiautomaticclassificationmanual.readthedocs.io/en/latest/

[15] Chavez, P.S. (1996) Image-Based Atmospheric Corrections—Revisited and Improved Photogrammetric Engineering and Remote Sensing. *American Society of Photogrammetry*, **62**, 1025-1036.

[16] Bueno, B. (2010) An Urban Weather Generator Coupling a Building Simulation Program with an Urban Canopy Model. Master's Thesis, Massachusetts Institute of Technology, Cambridge.

[17] Moro, J., Krüger, E. and Camboim, S. (2019) Metodologia para análise e quantificação de sombreamento proveniente de edificações de entorno sobre espaços públicos abertos. https://eventos.antac.org.br/index.php/encac/article/view/3960

[18] Callejas, I.J.A. (2012) Avaliação temporal do balanço de energia em ambientes urbanos na cidade de Cuiabá-MT. Ph.D. Thesis, Universidade Federal de Mato Grosso, Cuiabá.
https://ri.ufmt.br/bitstream/1/2530/1/TESE_2012_Ivan%20Julio%20Apolonio%20Callejas.pdf

[19] Ferreira, M., Oliveira, A. and Soares, J. (2011) Anthropogenic Heat in the City of São Paulo, Brazil. *Theoretical and Applied Climatology*, **104**, 43-56.
https://doi.org/10.1007/s00704-010-0322-7

[20] Oke, T.R. (1988) The Urban Energy Balance. *Progress in Physical Geography*, **12**, 471. https://doi.org/10.1177/030913338801200401

[21] Angelini, L.C., Fausto, M.A., Mutzenberg, D., Nassarden, D., *et al.* (2015) Relação entre albedo e temperatura da superfície estimados por sensoriamento remoto na área urbana de Cuiabá, Mato Grosso.
http://www.dsr.inpe.br/sbsr2015/files/p0377.pdf

[22] Muniz-Gäal, L.P., Pezzuto, C.C., de Carvalho, M.F.H. and Mota, L.T.M. (2018) Parâmetros urbanísticos e o conforto térmico de cânions urbanos: O exemplo de Campinas, SP. *Ambiente Construído*, **18**, 177-196.
https://doi.org/10.1590/s1678-86212018000200249

[23] Aldawi, F., Alam, F., Khan, I. and Allghamdi, M. (2013) Effect of Climates and Building Materials on House Wall Thermal Performance. *Procedia Engineering*, **56**, 661-666. https://doi.org/10.1016/j.proeng.2013.03.175

[24] Costa Neto, P.L. (2002) De O Estatística Básica. Edgard Blücher, São Paulo.